

# We are IntechOpen, the world's leading publisher of Open Access books Built by scientists, for scientists

6,900

Open access books available

186,000

International authors and editors

200M

Downloads

Our authors are among the

154

Countries delivered to

TOP 1%

most cited scientists

12.2%

Contributors from top 500 universities



WEB OF SCIENCE™

Selection of our books indexed in the Book Citation Index  
in Web of Science™ Core Collection (BKCI)

Interested in publishing with us?  
Contact [book.department@intechopen.com](mailto:book.department@intechopen.com)

Numbers displayed above are based on latest data collected.  
For more information visit [www.intechopen.com](http://www.intechopen.com)



---

# $\beta$ -Carotene and Free Radical Reactions with Nitrogen Oxides

---

Sara N. Mendiara and Luis J. Perissinotti

Additional information is available at the end of the chapter

<http://dx.doi.org/10.5772/67683>

---

## Abstract

The following presentation is based on experimental work we have already developed and published. We investigated the nitrogen oxides in different solvents and analyzed their reaction with  $\beta$ -carotene. The electron paramagnetic resonance spectroscopy (EPR) and ultraviolet and visible (UV-vis) spectroscopy were applied to investigate the reaction of  $\beta$ -carotene with nitrogen dioxide and nitric oxide in both pure dioxane and dioxane/water solvent. Free radicals were detected and evaluated with the EPR technique, which is highly selective and sensitive. A reaction mechanism was proposed on the basis of the experimental kinetic and EPR results. The validity of the mechanism was checked by applying simulation set up conditions that reproduced the results achieved. The radical intermediates proposed in the reaction: the  $\beta$ -carotene neutral radicals and the cyclic nitroxide neutral radicals were theoretically studied. For that purpose, the density functional theory (DFT) level was applied, selecting the most suitable method, the unrestricted Becke-style 3-parameter with the Lee-Yang-Parr correlation functional (UB3LYP) and the 6-31G(d) basis sets (d orbital functions). We developed an appropriate discussion on the importance of carotenoids compounds and their reactions in biological media. Also, we evaluated the role and the possible reactions of nitroxide intermediates.

**Keywords:**  $\beta$ -carotene, EPR, neutral radicals, nitrogen dioxide, nitroxides

---

## 1. Introduction

The following presentation is based on experimental work we have already developed and published. We investigated the behavior of nitrogen oxides in different solvents and analyzed the reaction of nitrogen oxides with  $\beta$ -carotene.

The reaction of free radicals with carotenoids and the properties of the carotenoid-free radicals formed are of widespread interest because of their potential role in biological systems. We have

---

carried out our work only with  $\beta$ -carotene, an unsaturated and extensively conjugated hydrocarbon. In vitro studies had shown the potential of carotenoids to act as free-radical scavengers. Nitrogen oxides, such as nitric oxide (NO) and the nitrogen dioxide ( $\text{NO}_2$ ), constitute a source of free radicals; they are species that have an unpaired electron. It is expected that nitrogen oxides may react in some important way with carotenoids and their radical intermediates. It is important to note that in our preliminary investigations, when mixtures of NO and  $\text{NO}_2$  were added to certain organic purified compounds, compounds of the type of the nitroxides were detected using the technique of EPR [1].

Carotenoids are a family of pigmented compounds that are synthesized by plants and microorganisms but not animals. However, humans and primates accumulate them in several tissues. Carotenoids are absorbed in the intestinal mucosa like other lipophilic components.  $\beta$ -carotene molecule is geared in the lipophilic membranes interacting, through van der Waals forces, with the hydrocarbon chains of the lipids [2–5]. Carotenoids can be traced in the cellular cytoplasm where they can interact with different components, including the nitrogen oxides. It is also important to take into account the metabolism of carotenoids;  $\beta$ -carotene is particularly hydrophobic and it is reasonable to hypothesize that it would need to be transformed to more polar compounds in order to be excreted via urine [6]. As well, lutein and  $\beta$ -carotene were measured in human brain tissue and related to better cognition in octogenarians. The protective effect may not merely be an antioxidant effect given that  $\alpha$ -tocopherol was less related to cognition than carotenoids [7]. The first report of the presence of  $\beta$ -carotene in the brain was in 1976, the patient was taking a high-dose  $\beta$ -carotene as a treatment and the carotenoid was measured within whole sections of the cerebrum [8].

We understood that the research might be quite profitable. The purpose of our work was to study and to enlighten the following problems:

- (a) The behavior of nitrogen oxides: NO and  $\text{NO}_2$  in some solvents (2001) [1].
- (b) The interaction and reaction among nitrogen oxides and  $\beta$ -carotene (2009) [9].
- (c) Theoretical evaluation of the intermediates proposed: the acyclic  $\beta$ -carotene neutral radicals, the acyclic nitrous  $\beta$ -carotene neutral radicals, and the cyclic nitroxide neutral radicals (2015) [10].

## 2. Development: (a), (b), and (c): conclusions and perspective

### 2.1. (a) The behavior of the nitrogen oxides NO and $\text{NO}_2$ in some solvents

Luckily, we had started the research developing a detailed study of solutions of nitrogen oxides in several solvents [1]. Those solutions were monitored with the following spectroscopic techniques: ultraviolet and visible (UV-vis) and electron paramagnetic resonance (EPR). The research allowed us to know what solvents can be used because they do not react with nitrogen oxides. We learned how to develop a careful control of the solvents. The knowledge acquired in this first work allowed us to follow, understand, and manage to clear up the

results later finally achieved from the  $\beta$ -carotene assays. Therefore, the solvent dioxane and other later used in our research were adequately tested. It was also verified that they did not react with the nitrogen oxides,  $\text{NO}_2$  and  $\text{NO}$ , even after prolonged times of observation in EPR (unlike what happened with hexane) [9].

$\text{NO}_2$  solutions were very carefully followed. In this chapter, we show only highlights from the developed research. Our first manuscript on nitrogen oxides, carried out in 2001, showed experimental and technical research in detail. **Figure 1** displays a set of EPR spectral records of the radical  $\text{NO}_2$  at environmental temperature. Solutions of  $\text{NO}_2$  were prepared in different

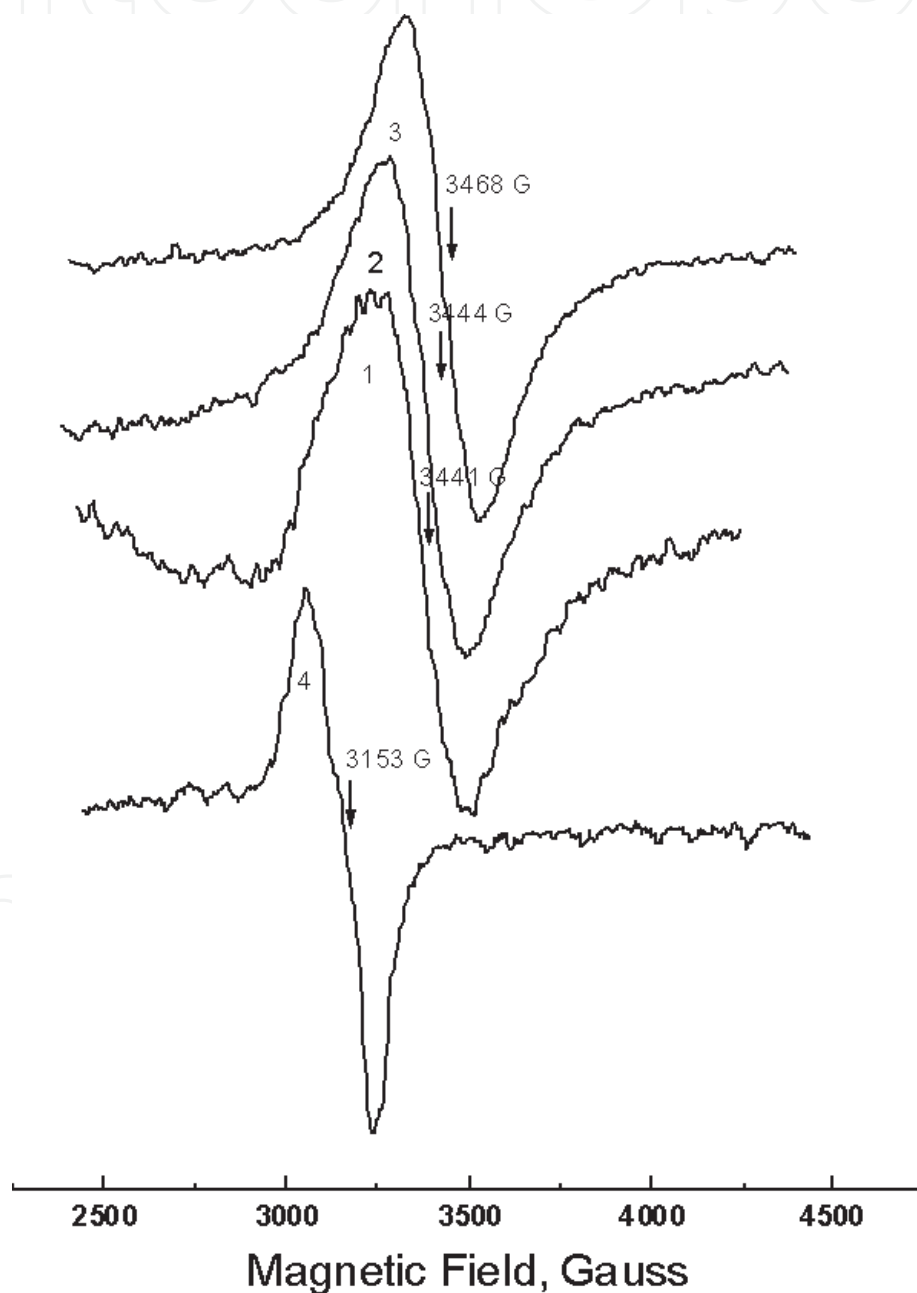


**Figure 1.** EPR spectra of  $\text{NO}_2$  at 290 K, in: (1) gas-phase; (2) hexane; (3) carbon tetrachloride; and (4) acetone. General instrumental settings: microwave power, 18,000 mW; attenuation, 9 dB; modulator frequency, 100 kHz; modulation amplitude, 2.5 G; time constant or response time, 0.2 s; scan rate, 200 s. The recipient was previously flushed with argon.

media: hexane, benzene, carbon tetrachloride, acetone, and water. You can see that each spectrum do not differ considerably from the others. The signal is not resolved, due to the movement of the free radical and to the collisions that usually take place at the working temperature. Noticed that our research was always carried out under argon atmosphere [1, 9].

In **Table 1**, we can see the values of  $g$ , the spectroscopic factor and of  $\Delta B$ , the total spectrum line width. Those data were extracted or calculated from **Figure 1**. We can also observe that the values in non-polar media are near the result measured in the gaseous phase. The general instrumental settings were microwave power, 18.000 mW; attenuation, 9 dB; modulator frequency, 100 kHz; modulation amplitude, 2.5 G; time constant or response time, 0.2 s; scan rate, 200 s.

We also prepared NO solutions. The preparation and handling of solutions of NO were performed under strict inert atmosphere. Even though precautions were employed to exclude oxygen from the system, a fingerprint UV-vis spectrum assigned to the presence of  $\text{NO}_2/\text{N}_2\text{O}_4/\text{HNO}_2$  as impurity was sometimes observed. UV-vis spectra of solutions of NO/ $\text{NO}_2$  in different solvents were analyzed. Those Spectra shown splits in some solvents. Some authors had interpreted them as the spectrum of NO [11]. However, it was confirmed that those UV-vis spectra were obtained in polar solvents and could be attributed to the formation of  $\text{HNO}_2$  [1, 12].

Usually, one has to control nitrogen dioxide samples, recording the UV-vis spectrum and the corresponding EPR spectrum. The EPR spectrum of  $\text{NO}_2$  is looked for in the following field interval: 1000–2000 Gauss, as you can observe in **Figure 1**. If we want to search for nitroxides, we must work in the following scan range: 50–200 Gauss. The EPR spectrum of NO was not detected in our field interval work.

When NO was dissolved in hexane, nitroxide intermediates were detected after 20 minutes or more, the radical was persistent. Probably no reaction took place when pure NO was present, but a trace amount of  $\text{NO}_2$  initiated the reaction [13, 14].

In 2003, we carried out the measurement of the  $\text{N}_2\text{O}_4$  dissociation constant ( $\text{N}_2\text{O}_4/2 \text{NO}_2$ ) in some solvents [15]. The  $\text{N}_2\text{O}_4$  dissociation constant measured in hexane, carbon tetrachloride,

Medium	$g^a$	$\Delta B$ , Gauss
Gas phase	1.999	1190 ± 58
Hexane	1.981	1194 ± 40
Benzene	1.985	563 ± 20
Carbon tetrachloride	1.978	897 ± 34
Acetone	2.185	499 ± 23
Water	2.176	502 ± 20

\*Results obtained in the present work. Instrumental settings are shown in **Figure 1**.

<sup>a</sup> $g$  values were determined with reference to a diphenylpicrylhydrazyl standard,  $g = 2.0036$ . The absolute errors are 0.002–0.004.

**Table 1.** EPR spectroscopic data of  $\text{NO}_2$  radical at 290 K: spectroscopic factor,  $g$ , and total line width,  $\Delta B$ .

and chloroform compares approximately with the values calculated by some previous authors [16–18]. The techniques usually applied were colorimetric and spectrophotometric ones. As the absorption along the appropriate wavelength range was small, the errors in measurements at low concentrations were considerably large. The EPR technique has also quantification errors; however, the method is more reliable and the radical is directly detected. As far as we were aware, this was the first attempt to measure this equilibrium with the EPR technique.

## 2.2. (b) The interaction and reaction among nitrogen oxides and $\beta$ -carotene: kinetic analysis and the corresponding modeling work

### 2.2.1. UV-vis measurements

$\beta$ -Carotene, a non-polar molecule, is insoluble in polar solvents like water. We desired to investigate the reaction of  $\beta$ -carotene with the nitrogen oxides generated in situ from aqueous solutions of sodium nitrite and sulfuric acid. In order to achieve our purpose, we prepared solutions of  $\beta$ -carotene in pure and adequately checked dioxane solvent, under argon atmosphere and constant temperature. The dioxane-water mixtures remained homogeneous and so the UV-vis spectroscopy studies could be applied. Other aprotic solvents easily cause cloudiness when water is added, then UV-vis measurements cannot be carried out.

### 2.2.2. EPR measurements

EPR measurements were carried out with the  $\beta$ -carotene solution in pure dioxane plus an aliquot of NO and NO<sub>2</sub> in pure dioxane. The solutions in dioxane had low concentration of the persistent radical, besides the triplet-type signal was recorded during 5 days. In pure dioxane, we only developed a qualitative approach. On the other hand, we could design a quantitative study carried out with  $\beta$ -carotene solution in pure dioxane plus an aliquot of the dioxane/water solution with the nitrogen oxides formed in situ from sodium nitrite in an acid medium. Also the formation and decay of the persistent intermediates was monitored and shown in **Figure 2**. Dioxane solvent was tested, and no EPR signal was detected even after prolonged times of observation.

### 2.2.3. Kinetic measurements

Kinetic measurements were developed in dioxane/water solvent at 298 K. All the measurements were successfully simulated with the software for chemical kinetics, following the reaction path proposed in **Figure 3**. In **Table 2**, each reaction was described and the corresponding kinetic constant assigned. Unfortunately, in our 2009 manuscript, the sixth equation had one mistake, we must write  $P_1$  instead of  $P_2$  [9]. In the 2015 manuscript, the rate constants  $k_i$  ( $i = 1$  to 7) were not written above the arrows [10].

In **Figure 3** and **Table 2**, we observed that whenever both NO and NO<sub>2</sub> were present, abstraction took place and nitroxides formed. Furthermore, it has already been shown that NO is less

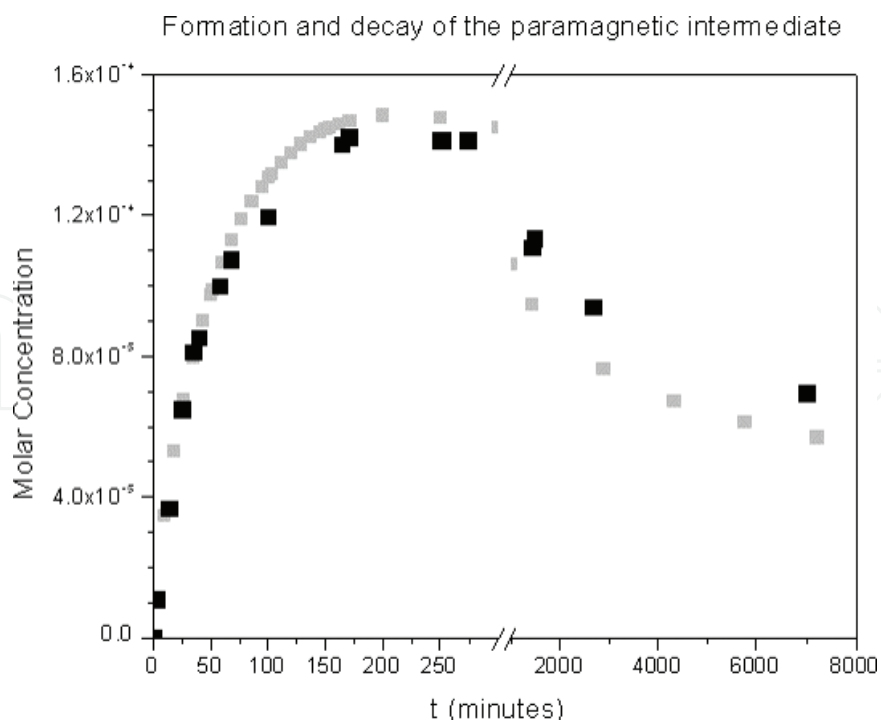


**Figure 2.** Formation and decay of a persistent type radical generated from a solution of  $\beta$ -carotene,  $1 \times 10^{-2}$ M, and nitrite anion,  $1 \times 10^{-1}$ M in dioxane:water ( $x_{\text{dioxane}} = 0.65$ ) and in the presence of an acid medium, pH = 2 at 298 K. The gray curve and symbols represent the values obtained from the kinetic simulation process; the black square symbols represent our experimental values. After 20 days, we were still able to measure a radical concentration of  $3.5 \times 10^{-5}$  M, not shown in the graph. The reactions were carried out under argon atmosphere.

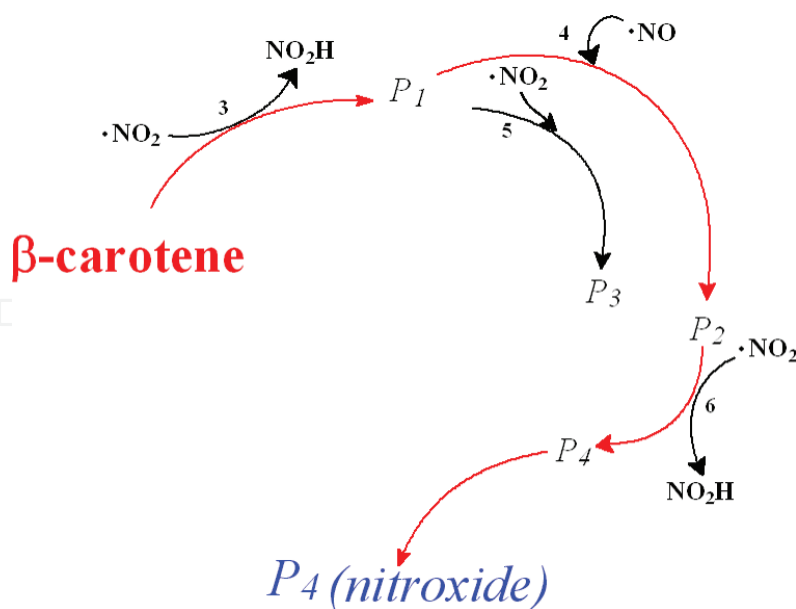


**Figure 3.** General reaction pathway proposed. The figure shows, in first place, the abstraction reactions of allylic hydrogens from  $\beta$ -carotene by nitrogen dioxide radicals and the formation of the products  $P_1$ .  $P_1$  represents different possible  $\beta$ -carotene neutral radicals.  $P_2$  represents the nitrous  $\beta$ -carotene formed with nitric oxide radicals.  $P_3$  represents the products formed with nitrogen dioxide radicals, not studied in this work.  $P_4$  represents the neutral radicals that are formed after the reaction of  $P_2$  with nitrogen dioxide radicals, another abstraction reaction of allylic hydrogens has taken place. Finally, when  $P_4$  generates an internal ring, a radical  $P_{4(\text{nitroxide})}$  comes up.

**Kinetic analysis in acid medium<sup>a</sup>**

$2NO_2H \xrightarrow{k_1} NO + NO_2 + H_2O$	$k_1 = 1.76 \times 10 \text{ M}^{-1}\text{s}^{-1}$
$NO + NO_2 + H_2O \xrightarrow{k_{-1}} 2NO_2H$	$k_{-1} = 3.01 \times 10^6 \text{ M}^{-1}\text{s}^{-1}$
$2NO_2 + H_2O \xrightarrow{k_2} NO_2H + NO_3^- + H^+$	$k_2 = 1.54 \times 10^6 \text{ M}^{-1}\text{s}^{-1}$
$\beta\text{-carotene} + NO_2 \xrightarrow{k_3} P_1 + NO_2H$	$k_3 = 4.7 \times 10^5 \text{ M}^{-1}\text{s}^{-1}$
$P_1 + NO \xrightarrow{k_4} P_2$	$k_4 = 1.0 \times 10^9 \text{ M}^{-1}\text{s}^{-1}$
$P_1 + NO_2 \xrightarrow{k_5} P_3$	$k_5 = 1.0 \times 10^9 \text{ M}^{-1}\text{s}^{-1}$
$P_2 + NO_2 \xrightarrow{k_6} P_4 + NO_2H$	$k_6 = 7.6 \text{ M}^{-1}\text{s}^{-1}$
$P_4 + P_4(\textit{nitroxide}) \xrightarrow{k_7} \textit{recombination; desproportionation}$	$k_7 = 2.5 \times 10^{-1} \text{ M}^{-1}\text{s}^{-1}$

<sup>a</sup>T = 298K.  $k_1$ ,  $k_{-1}$ , and  $k_2$  were already known. The rate constants  $k_4$  and  $k_5$  were considered diffusion controlled. The rate constants  $k_3$ ,  $k_6$ , and  $k_7$  were deduced from our modeling work. The kinetic simulation reproduced successfully the experimental kinetics results [9].

$P_1$  represents a possible allylic-type radical.  $P_2$  represents the possible isomers molecules of nitrous carotene.  $P_4$  represents the possible allylic-type radicals obtained from  $P_2$ . When a radical  $P_4$  cycles internally a radical  $P_4(\textit{nitroxide})$  is formed.  $P_3$  represents the products formed with nitrogen dioxide, not studied in this work.

**Table 2.** Reaction of β-carotene and nitrite in dioxane/water solution.

reactive and less efficient in the abstraction of a hydrogen atom than  $NO_2$  [9]. We can compare the following bond dissociation energies (BDE) values at 298 K:

- BDE (H-NO) =  $195.35 \pm 0.25 \text{ kJ}\cdot\text{mol}^{-1}$
- BDE (H- $NO_2$  or H-ONO) =  $327.6 \pm 2.1 \text{ kJ}\cdot\text{mol}^{-1}$

We proposed the formation of β-carotene neutral radicals that in the presence of nitrogen oxides, originated persistent radical intermediates. The reactions were carried out under argon atmosphere because of the reactivity of triplet oxygen; otherwise oxygenated compounds would be formed with the carotenoid neutral radicals.

We followed and measured the difficult kinetic of the mechanism proposed. The kinetic of the reaction depended on β-carotene, nitrite, and acid concentrations. We experimentally verified that the β-carotene followed a first-order decay and we measured the corresponding pseudo-first-order-constant [9].

In **Table 2**, a set of reactions represents the mechanism of the reaction. It is assumed that the system always behaves as if it has reached the acid-base balance.

$P_4$  was considered as  $P_4(\textit{nitroxide})$ . We ran a non-commercial simulation program of chemical kinetics. The validity of the proposed mechanism was therefore tested by numerical integration.

The values of  $k_1$ ,  $k_{-1}$ , and  $k_2$  were extracted from the literature. The rate constant  $k_3$  was adjusted following the UV-vis decay of  $\beta$ -carotene. The rate constants  $k_6$  and  $k_7$  were involved in the formation of the persistent radicals and were adjusted to the EPR results. The rate constants  $k_4$  and  $k_5$  were the recombination reactions between  $P_1$  radicals and nitrogen dioxide and nitric oxide radicals. We calculated the following values:  $k_4 = 1.4 \times 10^{10} \text{M}^{-1} \text{s}^{-1}$  and  $k_5 = 1.1 \times 10^{10} \text{M}^{-1} \text{s}^{-1}$ , by applying the equations of Smoluchowski, Stokes, and Einstein [19]. The calculations were developed taking into account the viscosity of the mixture dioxane-water,  $\eta_{25^\circ\text{C}} = 1.42 \times 10^{-3} \text{Pa}\cdot\text{s}$  and the molecular size of the NO,  $\text{NO}_2$  and  $\beta$ -carotene neutral radicals [20]. Actually, these constants were smaller because the nitrogen oxides reacted at some selected regions of the  $\beta$ -carotene neutral radicals. It was confirmed that changes of  $k_4$  and  $k_5$  in the order of  $10^7$  to  $10^{11}$  had no significant effect upon the simulation results, which match very well with our experimental results. So the value of  $1.0 \times 10^9 \text{M}^{-1} \text{s}^{-1}$  was selected and shown for  $k_4$  and  $k_5$  in **Table 2**.  $P_3$  represents the products formed with nitrogen dioxide, not studied in this work.

We considered that the nitrous acid was proportional to the nitrite anion through the acid-base equilibrium [9]. The simulation results at 298 K reproduced quite well the experimental decay of  $\beta$ -carotene in the range near the half-life at pH = 5.3. The formation and the decay of the persistent radical intermediate at pH = 2.2 were also very well reproduced. For example, we showed *Case (a)* and *Case (b)* through which we tested the experiments carried out.

*Case (a)* Initial concentrations:  $\beta$ -carotene,  $8.0 \times 10^{-6} \text{M}$ ; nitrite anion,  $9.3 \times 10^{-3} \text{M}$ ; pH, 5.3

The simulation program showed that the system achieved approximately the following steady state order of concentrations:  $[\text{NO}_2] \cong 10^{-8}$  to  $10^{-9} \text{M}$   $[\text{NO}] \cong 10^{-6}$  to  $10^{-7} \text{M}$   $[P_1] \cong 10^{-10} \text{M}$   $[P_2] \cong 10^{-6} \text{M}$

The pH achieved in the simulation run remained almost constant:  $5.30 \pm 0.02$ .

The maximum radical concentration reached was:  $[P_4 + P_{4(\text{nitroxide})}] \cong 10^{-11} \text{M}$ , in agreement with our EPR results.

The persistent radicals were not detected; evidently, our equipment had not enough sensibility.

*Case (b)* Initial concentrations:  $\beta$ -Carotene,  $1.0 \times 10^{-2} \text{M}$ ; nitrite anion,  $1.0 \times 10^{-1} \text{M}$ ; pH, 2.2.

The system achieved approximately the following steady state concentrations order:  $[\text{NO}_2] \cong 10^{-7} \text{M}$   $[\text{NO}] \cong 10^{-2} \text{M}$   $[P_1] \cong 0 \text{M}$   $[P_2] \cong 10^{-3} \text{M}$ .

The pH achieved in the simulation run remained almost constant:  $2.20 \pm 0.03$ .

The maximum radical concentration reached was:  $[P_4 + P_{4(\text{nitroxide})}] = 1.5 \times 10^{-4} \text{M}$ .

In agreement with our EPR results,  $1.4 \times 10^{-4} \text{M}$ , see **Figure 2**.

After 20 days, the kinetics simulation delivered a radical concentration of  $3.5 \times 10^{-5} \text{M}$  in perfect agreement with our experimental results.

We can observe that the examples have quite different experimental conditions; however, they both work with the same set of rate constants.

In **Figure 2**, the experimental measurement of the formation and decay of the radical intermediates was represented with black square symbols and the results from the kinetic simulation process were represented with gray symbols. **Figure 4** presents the recorded EPR spectrum of the radical intermediates. Although the spectrum may fit with a nitroxide-type radical showing a hyperfine coupling constant,  $a_N = 12.7$  G, the spectrum exhibits an increment in the central line. This central increment could be attributed to the contribution of a related allylic-type radical superimposed or to a set of related allylic-type radicals. However, the kinetic analysis generated poor concentrations for  $P_1$ , which represented the allylic radical intermediates. In addition, finally, with the aid of the computational methods, the hypothesis of the formation of cyclic nitroxides was favored [10].

### 2.3. (c) Theoretical evaluation of the intermediates proposed: the acyclic $\beta$ -carotene neutral radicals, the acyclic nitrous $\beta$ -carotene neutral radicals, and the cyclic nitroxide neutral radicals

The purpose of the following research was to unravel the structures of the related persistent intermediate or intermediates, we called them  $P_4$  (nitroxide) or cyclic nitroxide neutral radical or radicals.

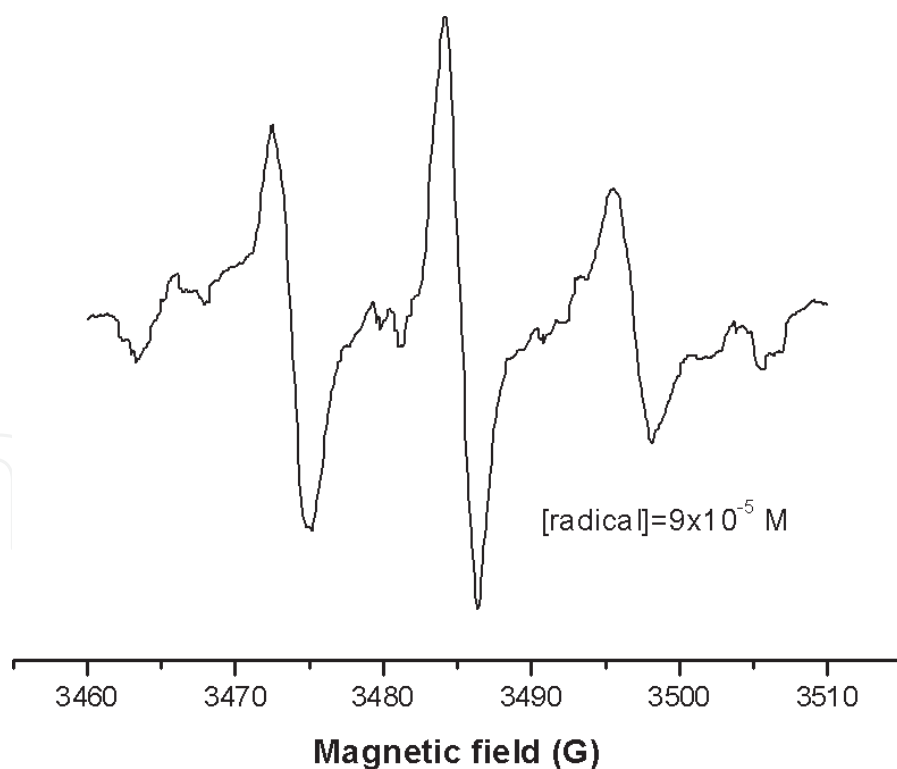


**Figure 4.** The figure shows a first-derivative X-band EPR spectrum of the intermediate called  $P_{4(\text{nitroxide})}$ , one or more type of persistent intermediate formed in the reaction of  $\beta$ -carotene with nitrite anion in acid medium (dioxane/water) at 298 K, under argon atmosphere. Spectrometer settings: microwave frequency, 9.92 GHz; modulation frequency, 100 kHz; microwave power, 11.3 mW; attenuation, 10 dB; field modulation, 0.125 G; receiver gain,  $2 \times 10^5$ ; time constant, 0.05 s; scan range, 50 G; scan time, 5 s. The peak-to-peak value is of 12.7 Gauss and  $g = 1.994$  [9].

On the basis of the kinetic studies, it was reasonable to propose intermediates of the nitroxide type. In a biological medium, one can expect that species react with each other. Or hope that radicals from  $\beta$ -carotene react with neighboring molecules of nitrous carotenes generating acyclic nitroxides. However, in the dilute solutions of  $\beta$ -carotene, where the reactions with the nitrogen oxides were carried out, the radicals kept away and intra-radical reactions would preferably take place. Thus, on that account, we considered it suitable to propose the formation of the rings.

We looked for the help of the computational and theoretical methods in order to study and compare the characteristics of the proposed structures and found out that the density functional theory (DFT) met the best conditions, given that it included the effects of electron correlation. DFT used very suitable approaches for energy exchange and for the correlation. The main conclusion was that for neutral radicals we could obtain good results with the approximate method Unrestricted Becke-style 3-parameter density functional theory using the Lee-Yang-Parr correlation functional (UB3LYP), both for the calculation of the energy of the system and for the calculation of the hyperfine coupling constants (hfccs). The selected basis sets, that used *d orbital functions*, allowed a good resolution, with an adequate cost of time, with a personal computer. The software used allowed to obtain the values of energy of each structure, which permitted to evaluate the relative stability of the radicals. Also, the software provided us the isotropic hfccs of each nucleus of the radical intermediates proposed [10].

Finally, the hfccs of the nuclei of hydrogen ( $^1\text{H}$ ) and nitrogen ( $^{14}\text{N}$ ) obtained with the theoretical methods allowed us to develop the simulation of the spectra that were experimentally recorded, like that shown in **Figure 4**.

Different possible rings with 3, 5, 6, 7, or 8 atoms were built and tested. However, only with some of them the corresponding geometric optimizations were achieved. The radicals with cycles of five atoms were found to be the most favored and those of lower energy.

In the General Reaction Pathway proposed in **Figure 3**, the following intermediates were appreciated:

- *Allylic-type radicals,  $P_1$*
- *Nitrous allylic radicals,  $P_4$*
- *Cyclic nitroxides formed by internal cyclization of the nitrous allylic radicals,  $P_{4(\text{nitroxide})}$*

With the aim of avoiding confusion in the interpretations described, the process of formation of the radical intermediates follows.

- *Allylic-type radicals,  $P_1$*

**Figure 5** helps to visualize the possible allylic hydrogens of  $\beta$ -carotene (the characteristic atomic symbols (C, H) are usually not shown in this type of molecular representation). The set of neutral allylic radicals from  $\beta$ -carotene is symbolized by  $P_1$  in **Figures 3** and **6**.

The molecule of  $\beta$ -carotene has allylic hydrogens, which are hydrogen atoms of the methyl groups at positions 5 and 5'; 9 and 9'; 13 and 13'. Allylic-type radicals are obtained by the loss, by abstraction, of those hydrogen atoms:

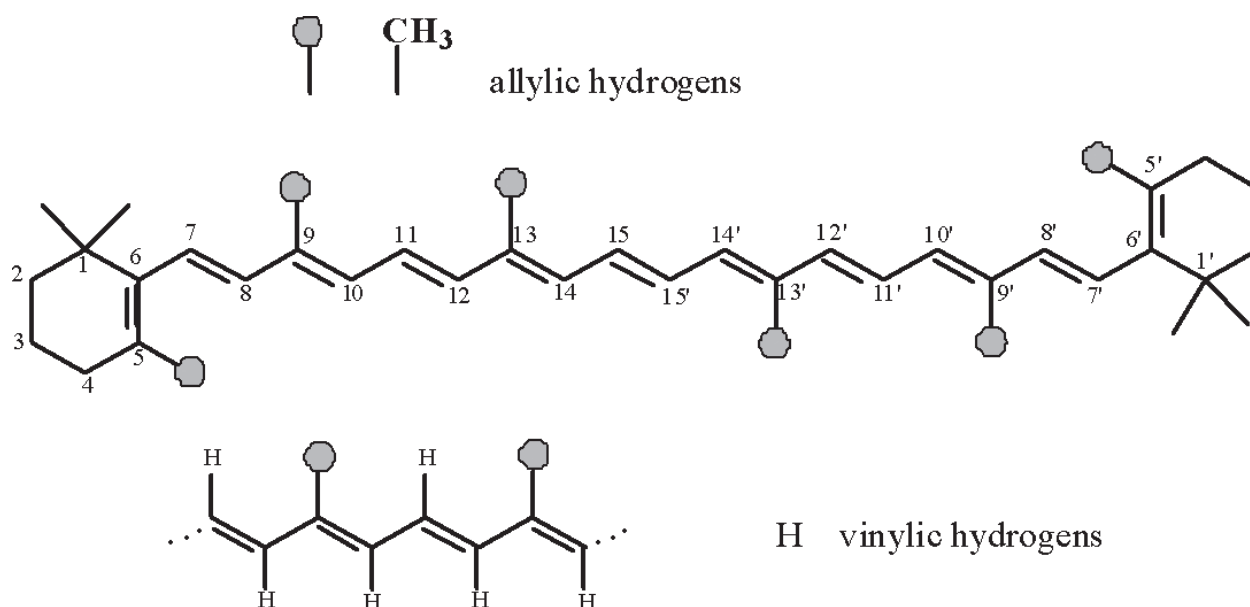


**Figure 5.** The molecule of β-carotene has allylic hydrogens, that are hydrogen atoms of the methyl groups at positions 5 and 5'; 9 and 9'; 13 and 13'. Vinylic hydrogen atoms are attached to the polyene chain at carbons: 7,8,10,11,12,14,15,15', 14',12',11',10',8', and 7'. Methyl groups with primary hydrogens, but not allylic type are represented with only a line or a bar in positions 1 and 1'.

$P_{10(5 \text{ or } 5')}$ : The allylic-type radical is formed by the loss of a hydrogen atom of the methyl attached to carbon 5 or 5'.

$P_{10(9 \text{ or } 9')}$ : The allylic-type radical is formed by the loss of a hydrogen atom of the methyl attached to carbon 9 or 9'.

$P_{10(13 \text{ or } 13')}$ : The allylic-type radical is formed by the loss of a hydrogen atom of the methyl attached to carbon 13 or 13'.

The molecule of β-carotene has also methyl groups (represented by a line or a bar) at positions 1 and 1'; they are primary hydrogen atoms. Those primary hydrogen atoms are not abstracted, they have higher bond energy than the allylic ones. In **Figure 5**, you can also appreciate the vinylic hydrogen atoms in the polyene chain. Those vinylic hydrogen atoms are attached to carbons: 7,8,10,11,12,14,15,15',14',12',11',10',8', and 7'; they have even higher bond energy than the primary hydrogen atoms. Observe that the radicals formed by the loss of allylic hydrogens are indeed stabilized by resonance.

In **Figure 6**, we followed the formation of the neutral carotenoid allylic radicals described below:

$P_{10(5 \text{ or } 5')}$ : The β-carotene loses an allylic hydrogen atom from the methyl group attached to position 5 or 5'. The conjugation effect formed a contributing resonance structure, an allylic tertiary radical on carbon 6 (see **Figure 5**), it is  $P_{11(5 \text{ or } 5')}$

$P_{12(5 \text{ or } 5')}$ : It is another contributing resonance structure with the unpaired electron in carbon 13'.

$P_{10(5 \text{ or } 5')}$ ,  $P_{11(5 \text{ or } 5')}$  and  $P_{12(5 \text{ or } 5')}$  are contributing resonance structures of the *same resonance hybrid*.

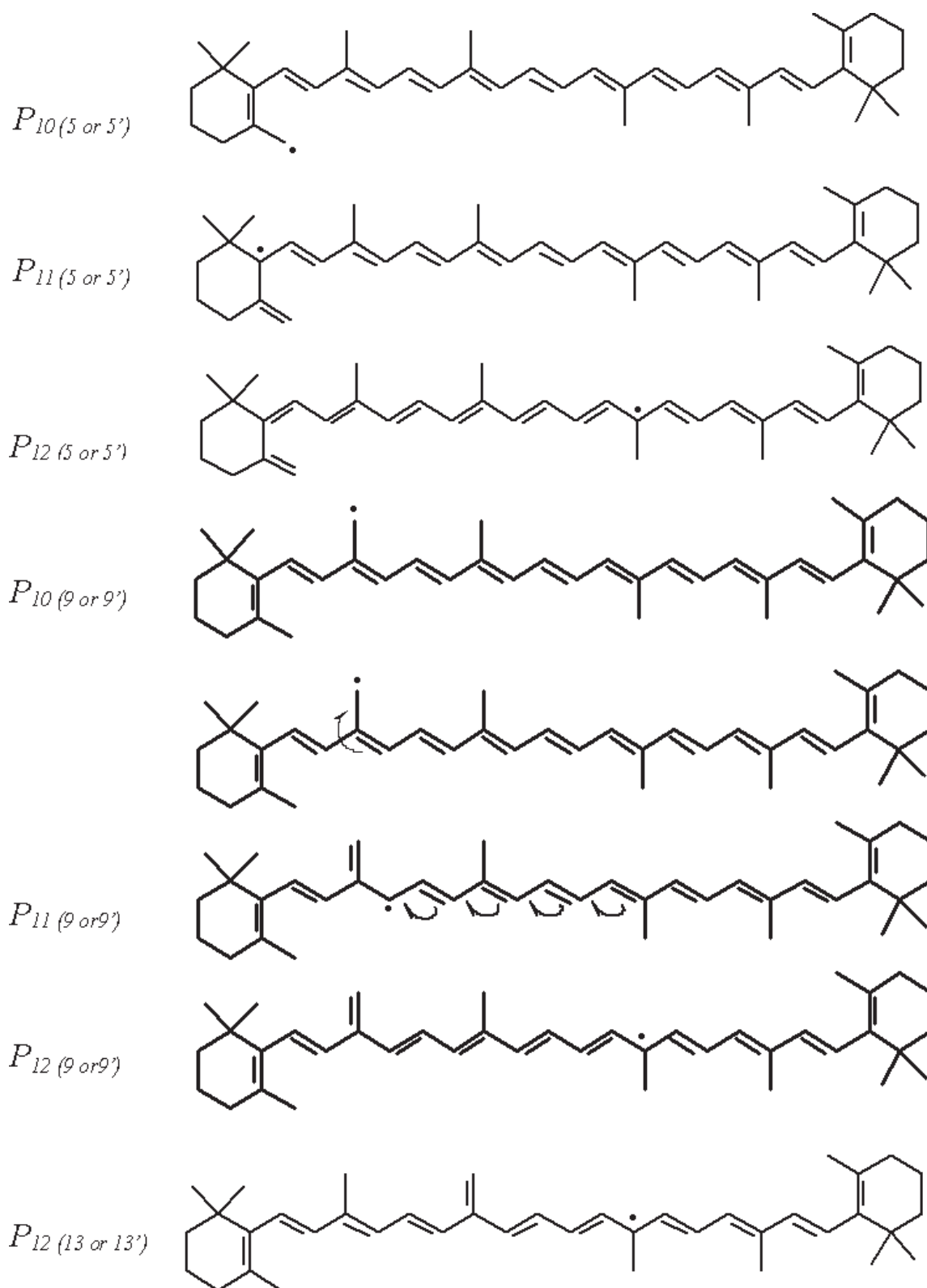


**Figure 6.** Several radicals of the allylic type are shown,  $P_i$ . There are three possibilities of allylic hydrogens:  $P_{10(5 \text{ or } 5')}$ ;  $P_{10(9 \text{ or } 9')}$ , and  $P_{10(13 \text{ or } 13')}$ . The second subscript indicates different contributing resonance structures, for example,  $P_{11(5 \text{ or } 5')}$  and  $P_{12(5 \text{ or } 5')}$ . The radical formed by the loss of a methyl hydrogen atom in position 9 or 9' is  $P_{10(9 \text{ or } 9')}$  observe that the electronic movements are shown in three related structures.  $P_{10(13 \text{ or } 13')}$  is the radical formed by the loss of a methyl hydrogen atom in position 13 or 13'. For this last case, only one possible structure is designed.

In the case of  $P_{10(9 \text{ or } 9')}$  the resonance or electronic movements are also shown. For  $P_{10(13 \text{ or } 13')}$  only one structure is designed.

- Nitrous allylic radicals,  $P_4$

The  $P_4$  radicals were also investigated with the theoretical methods:

- Some of them could not reach a geometric optimization presenting convergence failure.
- Other  $P_4$  radicals failed to reach the geometric optimization, expelling the NO group and regenerating the  $\beta$ -carotene molecule.
- In others, a radical was optimized geometrically but turned out to be a  $P_4(\textit{nitroxide})$ .
- Cyclic nitroxides formed by internal cyclization of the nitrous allylic radicals,  $P_{4(\textit{nitroxide})}$

In **Figure 7**, we appreciate that  $P_{12(5 \text{ or } 5')}$  is the intermediate that react with nitric oxide generating  $P_{22}$ , the nitrous allylic compound, see **Figure 3**.

$P_{22}$  loses by abstraction an allylic hydrogen atom from the methyl in position 9' generating  $P_{42}$ , the corresponding nitrous allylic radical and finally the formation of  $P_{42(\textit{nitroxide})}$ .

(**Figure 6** in our work of 2015 has an error; the nitroxide displayed is not generated from the listed precursors. The precursors designed would actually lead to another nitroxide not shown. The optimization of that nitroxide was completed on the basis of negligible forces. The stationary point was found but the convergence criteria were reached by only three of the required four cases [10]. In the present work, we have the opportunity of showing and solving the mistake. In **Figure 7**, we appreciate the precursors that actually lead to  $P_{42(\textit{nitroxide})}$ .)

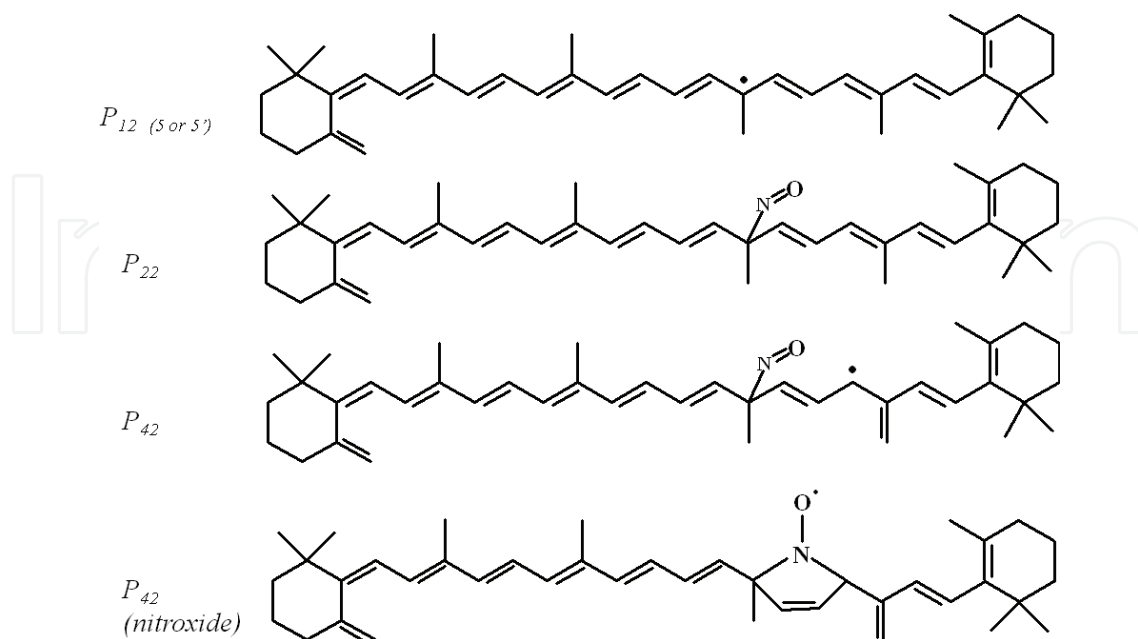


**Figure 7.** Formation of the cyclic  $P_{42(\textit{nitroxide})}$  from the allylic precursor. The tertiary allylic radical  $P_{12(5 \text{ or } 5')}$  is a contributing resonance structure of high weight.

In **Figure 8**, the optimized structure of  $P_{42}(\text{nitroxide})$  is displayed. Each atom is labeled with a number.

In order to carry out the simulation, three selected nitroxides were chosen, those of lower energy and those that best met the requirements for optimization. We selected two rings of five atoms ( $P_{41}(\text{nitroxide})$ ;  $P_{42}(\text{nitroxide})$ ) and one of eight atoms ( $P_{43}(\text{nitroxide})$ ).

We simulated quite satisfactorily the experimental recorded EPR spectrum in **Figure 4**, by adding the theoretical spectra of  $P_{42}(\text{nitroxide})$  from  $P_{12}(\text{5 or 5'})$  and  $P_{41}(\text{nitroxide})$  from  $P_{11}(\text{5 or 5'})$  both cyclic nitroxides of five atoms. Also we built another simulation by adding  $P_{42}(\text{nitroxide})$ ,  $P_{41}(\text{nitroxide})$  and  $P_{43}(\text{nitroxide})$  from  $P_{10}(\text{9 or 9'})$ , a cyclic nitroxide of eight atoms [10].

**Figure 9** shows the theoretical spectra and simulation of the persistent EPR recorded spectrum of **Figure 4**. In part (a), we may appreciate the theoretical EPR spectra of the nitroxides  $P_{41}(\text{nitroxide})$ ,  $P_{42}(\text{nitroxide})$ , and  $P_{43}(\text{nitroxide})$ . In order to simulate the experimental recorded spectra, one must add up the spectra of nitroxides, multiplying the values of  $P_{41}(\text{nitroxide})$  by the factor 1 and  $P_{42}(\text{nitroxide})$  by the factor 0.4 and multiply the values of  $P_{43}(\text{nitroxide})$  by the factor 0.2. Part (b) shows the sum that simulates quite well the experimental spectrum shown in **Figure 4**.

Simulations were also carried out considering the contribution of the  $\beta$ -carotene neutral radicals or allylic neutral radicals. It was observed that with less than 0.1 order factors, there were no appreciable changes, as is expected due to the result of the kinetic modeling. Although the  $\beta$ -carotene neutral radicals could be persistent, the nitroxide-type signal obtained would not be modified.

The theoretical spectra were built from the calculated isotropic hyperfine coupling constants. The hfccs values larger than 0.4 Gauss are shown in **Table 3**.

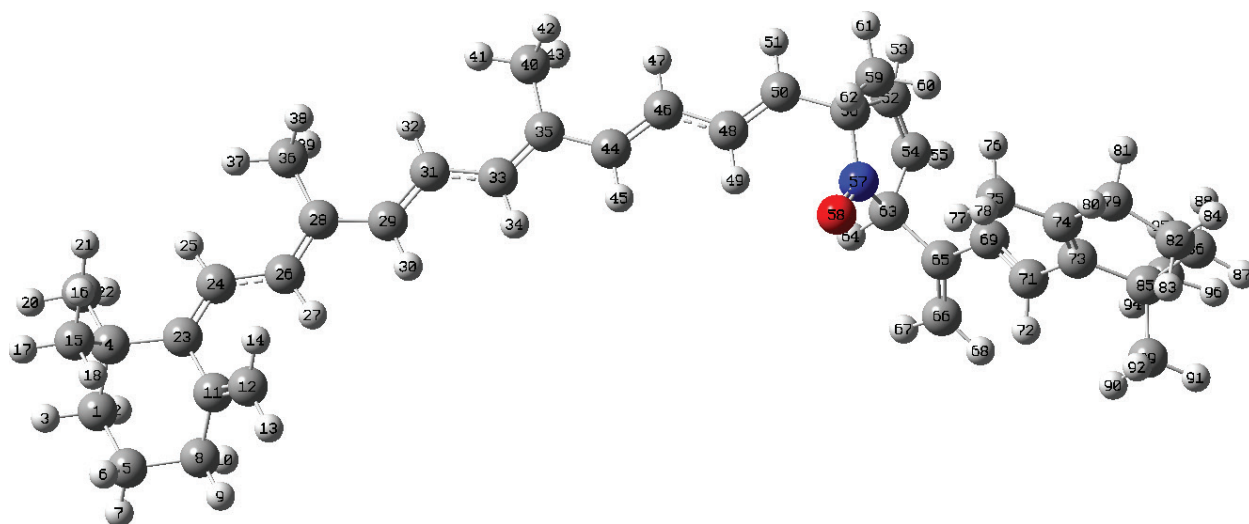


**Figure 8.** Visualization of the optimized geometric structure of the intermediate radical proposed in **Figure 7**:  $P_{42}(\text{nitroxide})$ .

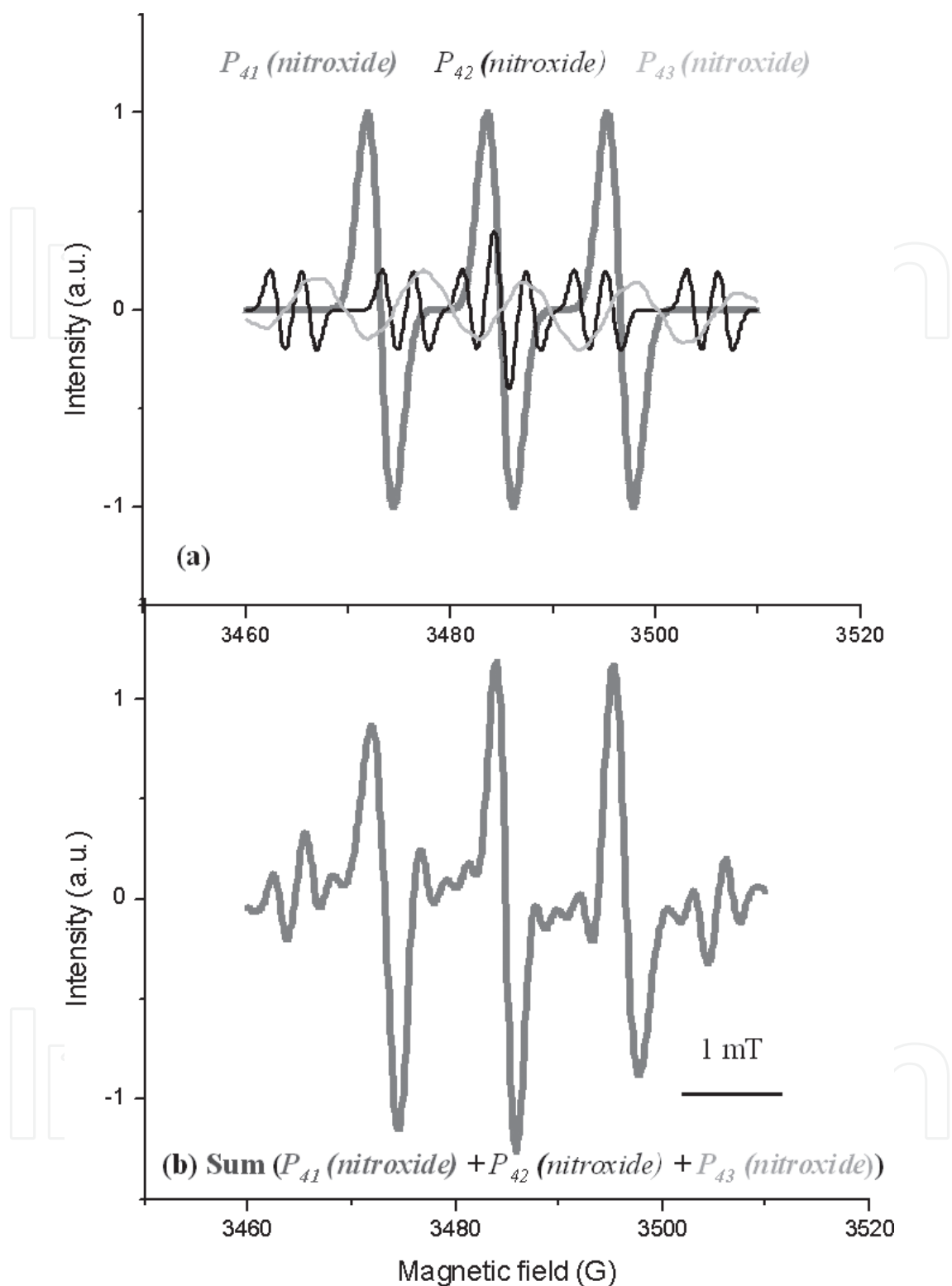


**Figure 9.** EPR theoretical spectra and simulation. In the part (a) the EPR theoretical spectra of the nitroxides are recorded:  $P_{41}(\text{nitroxide})$  in gray,  $P_{42}(\text{nitroxide})$  in black, and  $P_{43}(\text{nitroxide})$  in pale gray color. The values of  $P_{41}(\text{nitroxide})$  are multiplied by a factor of 1,  $P_{42}(\text{nitroxide})$  are multiplied by a factor of 0.4 and the values of  $P_{43}(\text{nitroxide})$  by a factor of 0.2. The part (b) shows the sum of the spectra in order to simulate the experimental spectrum. The peak-to-peak value is 12.1 Gauss, (10 Gauss  $\equiv$  1 mT). Data from Table 3 are used.

Nuclei	$P_{41}(\text{nitroxide})$	Nuclei	$P_{42}(\text{nitroxide})$	Nuclei	$P_{43}(\text{nitroxide})$
3 H	0.73171	49 H	0.42705	28 H	0.94710
10 H	0.91335	51 H	2.99147	31 H	0.45231
14 H	0.56426	53 H	-0.53599	53 H	2.00175
18 H	0.57683	55 H	-0.55714	54 H	9.42852
25 H	-0.53235	57 N	10.95771	56 H	19.03785
27 H	-0.58125	60 H	-0.45979	57 H	2.93589
29 N	11.68685	62 H	-0.60386	88 N	11.40254
33 H	-0.57914	64 H	18.74614	92 H	2.15932
34 H	-0.47031			96 H	1.59845
36 H	-0.42026				

<sup>a</sup>The hfccs values were obtained by applying the method of calculation B3LYP/6-31G (d) to the optimized geometries. The hfccs values larger than 0.4 Gauss are shown. Gaussian offers results in Gauss, 10 G = 1 mT.

$P_{41}(\text{nitroxide})$  and  $P_{42}(\text{nitroxide})$  are rings of five atoms.  $P_{43}(\text{nitroxide})$  corresponds to a ring of eight atoms. Each atom is labeled with a number, as in **Figure 8** for  $P_{42}(\text{nitroxide})$ .

**Table 3.** Isotropic hyperfine coupling constants (hfccs), cyclic  $P_4(\text{nitroxides})$ , (Gauss)<sup>a</sup>.

### 3. Conclusions and perspective

We have provided considerable information about the behavior of nitrogen dioxide in some solvents. Also, we followed the action of both NO<sub>2</sub> and NO over some organic compounds. Most relevant was the study of the reaction of both oxides with the β-carotene molecule.

It is important to highlight that two spectroscopic techniques were used: UV-vis and EPR. UV-vis is fundamental for the tracking of reagents, and EPR is essential for the monitoring of the radical intermediates.

Finally, we used the theoretical and computational methods that provided support to the characteristics of the intermediates. Calculations for β-carotene cyclic nitroxide intermediates, β-carotene allyl radicals, and nitrous β-carotene radical showed that the combination of the 6-31G(d,p) basis set and the B3LYP exchange-correlation functional provided a quite accurate description of the hfccs of the nuclei of hydrogen and nitrogen. The calculation of the hfcc for nitrogen nuclei (<sup>14</sup>N, nucleus) in the case of the nitroxide persistent radicals was particularly difficult. This problem with the nitroxides was investigated and finally deduced that the choice of the basis sets was very important. Especially the number and nature of *d orbital functions* must be taken into account [10].

β-Carotene or other carotenoids compounds would be in the lipid and anaerobic part of cells where the investigated reactions could take place. The β-carotene could be a convenient scavenger, acting as a protective agent in biological media. The cyclic persistent nitroxides may react by disproportionation giving rise to hydroxylated carotenoid compounds and nitrones.

Hydroxylated compounds can pass into the lymphatic system and be replaced by new molecules of  $\beta$ -carotene. The nitron is a new scavenger that will lead to a continuously replacement process [10]. It is important to remember that the persistent nitroxides are still present in solutions after 20 days with a concentration of  $3.5 \cdot 10^{-5}$  M [9].

On the other hand, the nitroxides may react differently. For example:

- (a)  $\beta$ -Carotene may not be a good radical trapping antioxidant but the nitroxide may be [21].
- (b) The combination of the carotenoids lutein or zeaxanthin and lipid-soluble nitroxides exerted strong synergistic protection against singlet oxygen-induced lipid peroxidation. The synergistic effect may be explained in terms of protection of the intact lutein or zeaxanthin structure by effective scavenging of free radicals by nitroxides [22].

Moreover, we can see that nitric oxide is generated in different types of cells. Neuronal nitric oxide synthase (nNOS) is constitutively expressed in specific neurons of the brain. In addition to brain tissue, nNOS has been identified in adrenal glands, in epithelial cells of various organs. In mammals, the largest source of nNOS in terms of tissue mass is in the skeletal muscle [23].

It might be expected that nitrogen oxides and non-polar carotenoids compounds have together an important biological function. Take into account that in carotenoids with a hydroxyl group, the reaction path may be surely different.

The isolation of the cyclic nitroxides described would also be very important.

## Author details

Sara N. Mendiara<sup>1\*</sup> and Luis. J Perissinotti<sup>1,2</sup>

\*Address all correspondence to: mendiar@gmail.com

1 Department of Chemistry, Faculty of Exact and Natural Sciences, National University of Mar del Plata, Mar del Plata, Buenos Aires, Argentina

2 Commission of Scientific Research of the Province of Buenos Aires (CIC), La Plata, Buenos Aires, Argentina

## References

- [1] Mendiara S, Sagedahl A, Perissinotti L. An electron paramagnetic resonance study of nitrogen dioxide dissolved in water, carbon tetrachloride and some organic compounds. *Appl. Magn. Reson.* 2001; 20: 275–287. doi:10.1007/BF03162326
- [2] Halliwell B, Gutteridge JMC. *Free radicals in biology and medicine*, 4th ed. New York: Oxford University Press; 2007. ISBN 978-0-19-856868-1

- [3] Möller M, Li Q, Lancaster Jr. J, Denicola A. Acceleration of nitric oxide autoxidation and nitrosation by membranes. *IUBMB Life*. 2007; 59: 243–248. doi:10.1080/15216540701311147
- [4] Gruszecki W, Strzałka K. Carotenoids as modulators of lipid membrane physical properties. *Biochim. Biophys. Acta*. 2005; 1740: 108–115. doi:10.1016/j.bbadis.2004.11.015
- [5] Rao A, Rao L. Carotenoids and human health. *Pharmacol. Res.* 2007; 55: 207–216. doi:10.1016/j.phrs.2007.01.012
- [6] Kopec R, Schwartz S. Carotenoid cleavage dioxygenase and presence of apo-carotenoids in biological matrices. In: Winterhalter P, et al. (eds) *Carotenoid Cleavage Products*. ACS Symposium Series. Washington, DC: American Chemical Society; 2013. pp. 31–41. doi:10.1021/bk-2013-1134.ch004
- [7] Johnson E, Vishwanathan R, Johnson M, Hausman D, Davey A, Scott T, Green R, Miller L, Gearing M, Woodard J, Nelson P, Chung H, Schalch W, Wittwer J, Poon L. Relationship between serum and brain carotenoids,  $\alpha$ -tocopherol, and retinol concentrations and cognitive performance in the oldest old from the Georgia centenary study. *J. Aging Res.* 2013; 2013: 7–10. doi:10.1155/2013/951786
- [8] Hammond B, Jr. Dietary carotenoids and the nervous system. *Foods*. 2015; 4: 698–701. doi:10.3390/foods4040698
- [9] Mendiara S, Baquero R, Katunar M, Mansilla A, Perissinotti L. Reaction of  $\beta$ -carotene with nitrite anion in a homogeneous acid system. An electron paramagnetic resonance and ultraviolet-visible study. *Appl. Magn. Reson.* 2009; 35: 549–567. doi:10.1007/s00723-009-0185-1
- [10] Mendiara S, Perissinotti L. Neutral radicals in the reaction of  $\beta$ -carotene with  $\text{NO}_2$  and NO: computational study and simulation of the EPR spectra. *Appl. Magn. Reson.* 2015; 46: 1301–1322. doi:10.1007/s00723-015-0732-x
- [11] Gabr I, Patel R, Symons M, Wilson M. Novel reactions of nitric oxide in biological systems. *J. Chem. Soc. Chem. Commun.* 1995; 1995: 915–916. doi:10.1039/C39950000915
- [12] Wolak M, Stochel G, Hamza M., van Eldik R. Aquacobalamin (Vitamin  $\text{B}_{12a}$ ) does not bind NO in aqueous solution. Nitrite impurities account for observed reaction. *Inorg. Chem.* 2000; 39: 2018–2019. doi:10.1021/ic991266d
- [13] Brown J, Jr. The reaction of nitric oxide with isobutylene. *J. Am. Chem. Soc.* 1957; 79: 2480–2488. doi:10.1021/ja01567a035
- [14] Rockenbauer A, Korecz L. Comment on conversion of nitric oxide into a nitroxide radical using 2,3-dimethylbutadiene and 2,5-dimethylhexadiene. *J. Chem. Soc. Chem. Commun.* 1994; 1994: 145. doi:10.1039/C39940000145
- [15] Mendiara S, Perissinotti L. Dissociation equilibrium of dinitrogen tetroxide in organic solvents: an electron paramagnetic resonance measurement. *Appl. Magn. Reson.* 2003; 25: 323–346. doi:10.1007/BF03166693

- [16] Cundall, J. Dissociation of liquid nitrogen peroxide. Part II. The influence of the solvent. *J. Chem. Soc. Trans.* 1895; 67: 794–811. doi:10.1039/CT8956700794
- [17] Gray, P., Rathbone, P. Dissociation of liquid dinitrogen tetroxide; Henry's law coefficients and entropies of solution, and the thermodynamics of homolytic dissociation in the pure liquid. *J. Chem. Soc.* 1958; 1958: 3550–3557. doi:10.1039/JR9580003550
- [18] Redmond T, Wayland B. Dimerization of nitrogen dioxide in solution: a comparison of solution thermodynamics with the gas phase. *J. Phys. Chem.* 1968; 72: 1626–1629. doi:10.1021/j100851a040
- [19] Moore J, Pearson R. *Kinetics and Mechanism*, 3rd ed. New York: John Wiley & Sons; 1981. 240 p. ISBN 0-471-03558-0
- [20] Geddes J. The fluidity of dioxane-water mixtures. *J. Am. Chem. Soc.* 1933; 55: 4832–4837. doi: 10.1021/ja01339a017
- [21] Ingold K, Derek A. Advances in radical-trapping antioxidant chemistry in the 21<sup>st</sup> century: a kinetics and mechanisms perspective. *Chem. Rev.* 2014; 114: 9022–9046. doi:10.1021/cr500226n
- [22] Zareba M, Widomska J, Burke J, Subczynski W. Nitroxide free radicals protect macular carotenoids against chemical destruction (bleaching) during lipid peroxidation. *Free Radic. Biol. Med.* 2016; 101: 446–454. doi:10.1016/j.freeradbiomed.2016.11.012
- [23] Förstermann U, Sessa W. Nitric oxide synthases: regulation and function. *Eur. Heart J.* 2012; 33: 829–837. doi:10.1093/eurheartj/ehr304

